

Eigenvalue-Based Techniques for Continuous Sensing Model in MIMO CR Networks

Adoniran Judson Braga

Department of Electrical Engineering
University of Brasilia, Brazil 70904-970
Email: jbraga@ene.unb.br

Rausley A. A. de Souza

National Institute of Telecommunications
Santa Rita do Sapucaí, Brazil 37540-000
Email: rausley@inatel.br

Dayan Adionel Guimarães

National Institute of Telecommunications
Santa Rita do Sapucaí, Brazil 37540-000
Email: dayan@inatel.br

Abstract—Many studies on cognitive radio (CR) networks have been carried out to maximize the CR throughput under the restriction of avoiding interference on primary user (PU) network. Aiming at a higher network throughput than in the classic approach, the concept of continuous sensing is used, where secondary receiving nodes are responsible for the spectrum sensing and decision about the presence of the PU while others secondary users (SU) transmit in the same sensed spectrum band. In this paper we compare, in a continuous sensing scheme, the performance of eigenvalue spectrum sensing techniques in a multiple sensor CR network. The soft Akaike information criterion (SAIC) achieves the best performance for detection of the PU signal when the SU signal is strong and the modified maximum eigenvalue detection performs better when the SU signal is weak.

I. INTRODUCTION

Nowadays, the use of the electromagnetic spectrum for communication is growing: new services emerge over time, while traditional services remain active occupying most of attractive bands for wireless communication. Because of this, there is a serious scarcity of spectrum to be managed by the scientific community and regulatory agencies. On the other hand, even though much of the useful radio spectrum is already allocated to conventional systems, studies [1]-[4] have demonstrated that the assigned spectrum is significantly underutilized around the world. Aiming at optimizing the space-time allocation of radio spectrum, cognitive radio is proposed as a solution [5]. The idea is simple: while the licensed user (PU) for a certain spectral band is not transmitting for any reason, this spectrum may be available for unlicensed users (SU), as long as this channel is released as soon as the PU attempts to use it again. Therefore, spectrum sensing [6] is the main functionality enabling the CR to use the best spectrum's opportunities without interfering with the operation of licensed users. To reach a better sensing performance, a lower probability of false alarm (P_{fa}) is desired to maximize the utilization of the available spectrum, whereas a higher probability of detection (P_d) is required to avoid interference with PU. Consequently, there is a natural tradeoff in CR technology between avoiding interference with primary network and improving throughput for the secondary network.

The sensing period must be long enough to achieve a required P_d and avoid harmful interference with the PU. However, a channel detection time (CDT) [7] is usually stated to limit the time during which a PU can withstand interference

before the CR system detects it. So, within the CDT period, the CR users are required to perform the sensing and transmission tasks. Thus, the longer the sensing time, the shorter the transmission time, reducing the throughput and increasing the delay for traffic in the secondary network. Such periodic transmission interruption can lead to an inefficient usage of the available spectrum, and, consequently, to a reduction in the CR network capacity. Solid studies [8]-[11] have been carried out to minimize the sensing time and maximize the CR throughput for a given interference constraint. However, these studies are based on the assumption that the CRs are required to stop transmitting to perform the spectrum sensing. The dynamic frequency hopping (DFH) method [12] changed the paradigm that the CR users are not able to perform the sensing and transmission at the same time. In this approach, during the CR transmission through a working channel, sensing is performed in parallel in other channels. After the CDT period, the CR switches the operation to the best channel recently sensed, and the band previously used is vacated. Hence, interruption is no longer required for sensing [12]. Even though the DFH method has demonstrated an important advantage of this parallel sensing approach over the traditional one, the problem that the channel being sensed cannot be used for data transmission by the CR still persists.

Generally, channels being sensed are not used for data transmission because the CR spectrum sensing has been treated as a conventional signal detection problem [8]. Thus, signal detection techniques have been rarely used with adaptations regarding the CR objectives. The authors in [13] have proposed a spectrum monitoring technique at the receiver based on error statistics to be performed prior the spectrum sensing. The increase of the error rate may be caused by the presence of the PU signal and then a spectrum sensing is triggered. This considerably reduces the sensing rate, increasing the throughput in the SU network. The monitoring technique achieves a good performance if the secondary-to-primary power ratio (SPPR) is not too high. In high SPPR scenarios, the presence of the PU signal may be hardly detected or mistaken with fading of the SU signal. The work [14] has come up with a continuous sensing method based on energy detection [15], where sensing is performed at the receiving node of the SU. Thus, the SU at the transmitting node can keep transmitting as the primary user is idle, seeking a higher throughput in the SU system and continuity in sending data (thereby reducing the overhead). However, since the SU is allowed to transmit

while the spectrum is sensed, its signal becomes an intrinsic interferer in the task of sensing the PU.

We investigate the performance of six eigenvalue-based sensing schemes using the MIMO channel model adapted for the continuous sensing model with centralized sample processing at the fusion center (FC). In this study, the models and the FC concept can be employed in a centralized cooperative sensing system with several receivers or in a single receiver system with multiple sensors. Specifically, we assess the performance of the eigenvalue-based altered generalized likelihood ratio test (AGLRT); the altered maximum-minimum eigenvalue detection (AMMED); the altered maximum eigenvalue detection (AMED); and the altered energy detection (AED) [16]. Although the ED is not an exclusively eigenvalue-based detection technique, it can be implemented using eigenvalue information for the sake of completeness. We also analyse the performance of the model order estimator named AIC [17], and introduce a new technique based on it named soft Akaike information criterion (SAIC), which proved useful in low primary-to-secondary power ratio (PSPR) scenarios.

The remainder of this paper is organized as follows. Section II presents the modified system model for the eigenvalue-based sensing techniques in the presence of the secondary user, and Section III describes the AIC based techniques. Section IV describes the simulation setup, and Section V presents simulation results and discussions concerning the different techniques and PSPR. This paper ends with conclusions and suggestions for new research in Section VI.

II. EIGENVALUE-BASED SPECTRUM SENSING

In what concerns the baseband linear discrete-time MIMO fading channel model, assume that there are m sensors (e.g., antennas) in a CR, or m single-sensor CRs, each one collecting n samples of the received signal from p primary transmitters and q secondary transmitters during the sensing period, with $p + q < m$. Consider that these samples are arranged in a matrix $\mathbf{Y} \in \mathbb{C}^{m \times n}$. Similarly, consider that the transmitted signal samples from the primary and secondary transmitters are arranged in a matrix $\mathbf{X} \in \mathbb{C}^{p \times n}$ and in a matrix $\mathbf{S} \in \mathbb{C}^{q \times n}$, respectively. The PU and SU signals are i.i.d. (independent and identically distributed) random process and independent of each other. Let $\mathbf{H}_x \in \mathbb{C}^{m \times p}$ be the channel matrix with elements $\{h_{ij}\}$, $i = 1, 2, \dots, m$ and $j = 1, 2, \dots, p$, representing the channel gain between the j -th primary transmitter and the i -th sensor (antenna or receiver) and let $\mathbf{H}_s \in \mathbb{C}^{m \times q}$ be the channel matrix with elements $\{h_{ij}\}$, $i = 1, 2, \dots, m$ and $j = 1, 2, \dots, q$, representing the channel gain between the j -th secondary transmitter and the i -th sensor. Finally, let $\mathbf{V} \in \mathbb{C}^{m \times n}$ be the matrix containing thermal noise that corrupts the received signal. The matrix of collected samples is then

$$\mathbf{Y} = \mathbf{H}_x \mathbf{X} + \mathbf{H}_s \mathbf{S} + \mathbf{V}. \quad (1)$$

In eigenvalue-based sensing, spectral holes are detected using test statistics based on the eigenvalues of the sample covariance matrix of the received signal matrix \mathbf{Y} . If a multi-sensor device is used to decide upon the occupation of a given channel in a non-cooperative fashion, or even in a centralized

cooperative multi-node scheme with data-fusion [18], matrix \mathbf{Y} is formed, and the sample covariance matrix

$$\mathbf{R} = \frac{1}{n} \mathbf{Y} \mathbf{Y}^\dagger \quad (2)$$

is estimated, where $(\cdot)^\dagger$ means complex conjugate and transpose. From \mathbf{R} , the eigenvalues $\{\lambda_1 \geq \lambda_2 \geq \dots \geq \lambda_m\}$ are computed and the test statistics for the AGLRT, the AMMED, the AMED, and the AED may be calculated [16]. The decision performance depends on the decision distance between the \mathcal{H}_0 state, when PU signal is absent, and \mathcal{H}_1 , when PU signal is present. Assuming single primary and secondary transmitters ($p = q = 1$), these adapted tests are respectively calculated according to:

$$T_{\text{AGLRT}} = \frac{\lambda_1 + \lambda_2}{\frac{2}{m-2} \sum_{i=3}^m \lambda_i}, \quad (3)$$

$$T_{\text{AMMED}} = \frac{\lambda_1 + \lambda_2}{2\lambda_m}, \quad (4)$$

$$T_{\text{AMED}} = \frac{\lambda_1 + \lambda_2}{2P_{\mathcal{H}_0}}, \quad (5)$$

$$T_{\text{AED}} = \frac{\|\mathbf{Y}\|_F^2}{mnP_{\mathcal{H}_0}} = \frac{\sum_{i=1}^m \lambda_i}{mP_{\mathcal{H}_0}}, \quad (6)$$

where $\|\cdot\|_F$ is the Frobenius norm of the underlying matrix, and $P_{\mathcal{H}_0}$ is the SU signal (from the transmitting node) plus noise power averaged over all sensors.

For the conventional approach, all the eigenvalue based methods rely on the fact that the covariance matrix in the presence of white noise only is a diagonal matrix with all its elements equal to the thermal noise power σ^2 . However, when the PU signal arrives, the flat distribution of eigenvalues turns into a non-flat vector of eigenvalues with p stronger terms, and these methods try to assign the \mathcal{H}_1 channel state using this contrast. In the continuous sensing approach, the eigenvalue distribution is not flat prior the arrival of the PU signal, since the SU is transmitting. Consequently, there is a shorter decision distance between the \mathcal{H}_0 and \mathcal{H}_1 states, which worsens the decision performance for the four methods. In principle, this fact may discourage the continuous sensing approach since this system is worse when compared in equal conditions to the classic approach. However, this system is flexible in terms of sensing time, allowing for better sensing performance [14].

As one can see in (3), in AGLRT we calculate the ratio between the average of the two larger eigenvalues and the average of all the remaining eigenvalues. In AMMED we consider the ratio between the average of the two largest eigenvalues and the smallest eigenvalue. In AMED we compare the average of the two largest eigenvalues with $P_{\mathcal{H}_0}$, while in the AED the average of all eigenvalues is compared with $P_{\mathcal{H}_0}$. In AMED and AED, the thermal noise power σ^2 is assumed to be known and the same in each sensor input with uncorrelated samples, and the SU signal power can be estimated using a pilot channel [19].

III. SOFT AKAIKE INFORMATION CRITERION - SAIC

Considering complete uncorrelation between all PU signals and SU signals and full rank matrices \mathbf{H}_x and \mathbf{H}_s , for sufficiently large PU and SU signal-to-noise ratios, the smallest $m - (p + q)$ eigenvalues of \mathbf{R} will be noticeable smaller than the remaining $p + q$ ones [17]. Therefore, this composition indicates that the eigenvalues with the smallest indexes represent the most relevant components of the signal. Thus, it is possible to apply an algorithm in order to determine the number of relevant eigenvalues.

The Akaike information criterion (AIC) is used to select the necessary number of components to describe a signal without loss of information. It is a mathematical criterion based on information theory, in which given a set of candidate models for a data, the preferred model is the one with the minimum AIC value, where the AIC value is given by [17]

$$\text{AIC}[k] = -n(m - k) \ln \left[\frac{G_{m-k}}{A_{m-k}} \right] + k(2m - k), \quad (7)$$

where $k = 0, 1, \dots, m - 1$ is the index of the considered component, G_{m-k} and A_{m-k} are the geometric mean and the arithmetic mean of the $m - k$ smallest eigenvalues. After finding the value of k , named here as k_{\min} , that minimizes (7), it is possible to find the model order, which is given by

$$T_{\text{AIC}} = m - k_{\min} - 1. \quad (8)$$

The outputs of each test (decision variable) presented in the Section II are random variables with continuous probability density functions (PDF) and continuous intersection between their histograms for the \mathcal{H}_0 and \mathcal{H}_1 states. Therefore, the receiver operating characteristic (ROC) curves vary smoothly, due to the random nature of the noise and channel. In the case of the AIC, the outputs of each test for the states \mathcal{H}_0 and \mathcal{H}_1 is, when it correctly estimates the number of transmitters, equal to q and $p + q$ sources, respectively. This binary outcome is efficient when the signal SU does not exist or is very strong, but degrades P_d regardless of P_{fa} when weak signals may be seen as one or confused with noise. Since there are few discrete possible outputs, the error is more punitive. Soft Akaike information criterion (SAIC), introduced here, tries not to use only the minimum of $\text{AIC}[k]$ to decide for k_{\min} , but the whole vector weighted as

$$T_{\text{SAIC}} = \frac{\sum_{k=0}^{m-1} \frac{k}{\text{AIC}[k]^m}}{\sum_{k=0}^{m-1} \frac{1}{\text{AIC}[k]^m}}. \quad (9)$$

Differently from T_{AIC} , T_{SAIC} is not limited to integer numbers or discrete histogram, but non negative real numbers ensuring approximately continuous PDF.

IV. SIMULATION SETUP

The simulation setup under the discrete-time MIMO model considers that $\mathbf{Y} = \mathbf{H}_x \mathbf{X} + \mathbf{H}_s \mathbf{S} + \mathbf{V}$ is available to the FC. Matrices \mathbf{X} , \mathbf{S} , \mathbf{H}_x , \mathbf{H}_s , and \mathbf{V} are generated as follows: To simulate Gaussian distributed noise-like transmitted signals, \mathbf{X} and \mathbf{S} are formed by i.i.d. zero mean complex Gaussian samples. The choice for the Gaussian distribution is adopted because it accurately models several modulated signals, such as orthogonal frequency-division multiplexing (OFDM) with a

large number of subcarriers, which is the preferred modulation technique in most modern wireless technologies, including several digital television standards.

The elements in the channel matrices \mathbf{H}_x and \mathbf{H}_s are zero mean i.i.d. complex Gaussian variables that simulate a flat Rayleigh fading channel between each transmitter and sensor (CR), assumed to be constant during a sensing period and independent from one period to another. Although channel coefficients change in time and space, the average channel gain over all sensors or receivers is considered constant in time. Therefore, P_d and P_{fa} considered in this study are averaged values in flat Rayleigh fading channel. The entries in \mathbf{V} are unitary variance (unitary power), i.i.d. zero mean complex Gaussian variables that represent the additive thermal noise corrupting the received samples. The power of PU and SU signals are given by their signal-to-noise ratios, i.e. SNR_x and SNR_s , respectively, since noise has unitary variance.

The covariance matrix \mathbf{R} is computed from the received matrix \mathbf{Y} , and then the eigenvalues $\{\lambda_i\}$, $i = 1, 2, \dots, m$. The test statistics for the AGLRT, the AMMED, the AMED, the AED, the AIC and the SAIC are respectively computed from Equations (3)–(6), (8) and (9). In each detection technique, the corresponding test statistic is compared with a threshold computed from the desired false alarm probability, and a final decision upon the occupancy of the sensed channel is reached.

V. SIMULATION RESULTS

In this section we present simulation results and discussions concerning the influence of noise and SU signal on the performance of PU signal detection for the AGLRT, the AMMED, the AMED, the AED, the AIC, and the SAIC. The ROC curves shown hereafter were obtained with a minimum of 5,000 runs in Monte Carlo simulations implemented according to the setup described in Section IV. System parameters are those in Table I, unless otherwise indicated.

TABLE I. REFERENCE SYSTEM PARAMETERS.

PU signal-to-noise ratio	$\text{SNR}_x = -10$ dB
SU signal-to-noise ratio	$\text{SNR}_s = -\infty, -10, -5, 0, 5, 10$ dB
Number of primary transmitters	$p = 1$
Number of secondary transmitters	$q = 1$
Number of sensors	$m = 6$
Number of samples collected by each sensor	$n = 50$

The choice for a small SNR of the PU signal (-10 dB) is made to represent a more degrading, but yet realistic, situation from the perspective of spectrum sensing performance. For instance, IEEE 802.22 requires that the presence of digital TV transmissions should be sensed with 0.9 detection probability with a sensitivity of -114 dBm, which may be translated into very low SNR levels [20].

Figs. 1–5 show the ROC curves relating P_{fa} and P_d for the AGLRT, the AMMED, the AMED, the AED, and the SAIC. No curves for the AIC is shown, since the discrete values of T_{AIC} cause intolerable errors in scenarios with strong noise, as explained in Section III. It can be seen that the classical sensing scheme, i.e. when no SU signal is present, outperforms the continuous sensing model in all techniques. As shown in [14], the strength of the continuous sensing model is the time flexibility, since it is not necessary to stop sensing to transmit.

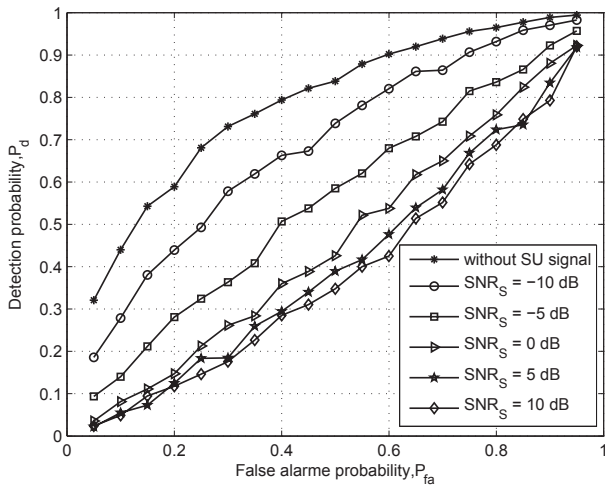


Fig. 1. ROC curves for the AGLRT under variations of SU SNR.

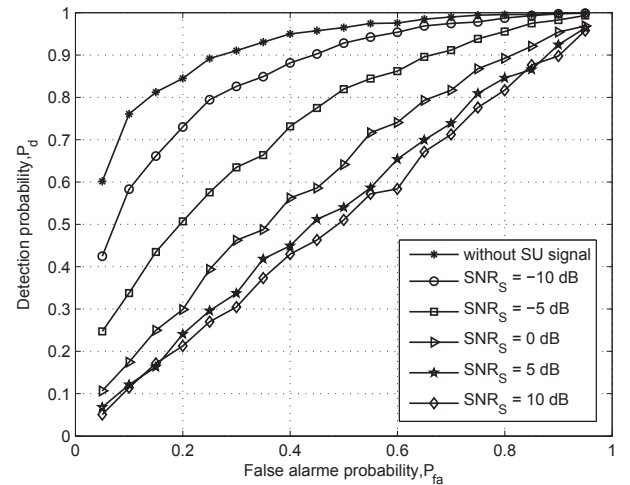


Fig. 3. ROC curves for the AMED under variations of SU SNR.

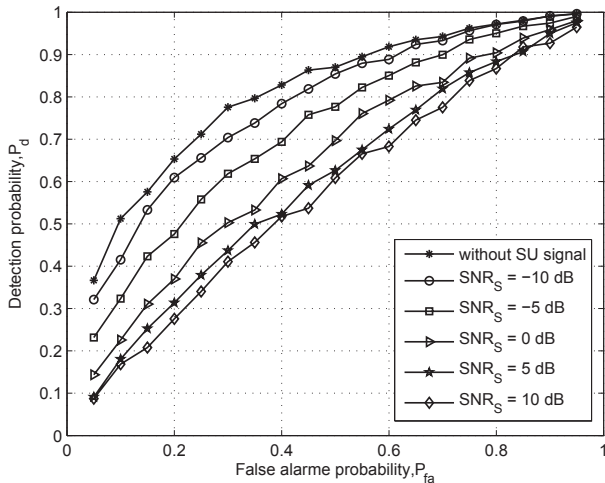


Fig. 2. ROC curves for the AMMED under variations of SU SNR.

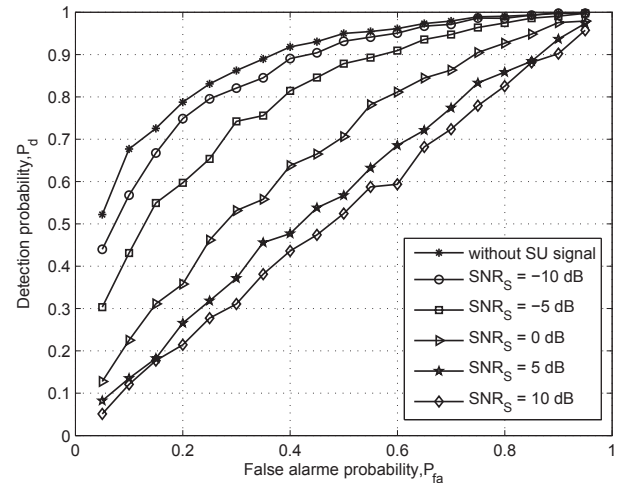


Fig. 4. ROC curves for the AED under variations of SU SNR.

It means that, for a fixed bandwidth, a much bigger number of samples can be used to enhance P_d as a function of a longer sensing time. However, one should be aware of the channel coherence time and bandwidth waste in transmitting samples to the FC.

Comparing the methods for the classical model, the AED and the AMED, where the noise variance is assumed to be known, perform better than the others, with a slight advantage to the AMED. However, with the presence of the SU signal, the performance of the AED exceeds slightly the AMED, even though both show a growing deficiency as a function of the SU signal power. As we can see, the AMMED performs better than the AGLRT. However, a more practical comparison is made in Fig. 7 where P_{fa} and P_d are set to values of more practical meaning.

In Fig. 5 we see an atypical behavior in the SAIC curves as a function of SNR SU. The worst results are not from curves with high SNR SU, but those in which the secondary user

signal is active and has low power. For curves with SU SNR equal to 0, 5 and 10 dB, the SAIC achieved the best results. This is due to the fact that, for the first four techniques, the goal is to detect the presence of the PU signal under the interference of the SU signal. However, for SAIC and the AIC, the number of transmitting sources is taken into account.

Another way to compare the detection methods is to compute the effort required to arrive at a certain target performance. Here, we tested the number of samples required to achieve a probability of detection of 90% when the probability of false alarm do not exceed 10%, considering low PU signal power ($SNR_X = -10$ dB) and high SU signal power ($SNR_S = 0$ dB). The other parameters remain as in Table I. The results are depicted in Fig. 6.

For the sake of comparison, we show in Fig. 7 the curves of P_d as a function of the number of samples when no SU signal is present. As expected, we see clearly that the number of samples required to achieve $P_d = 90\%$ is always less than in

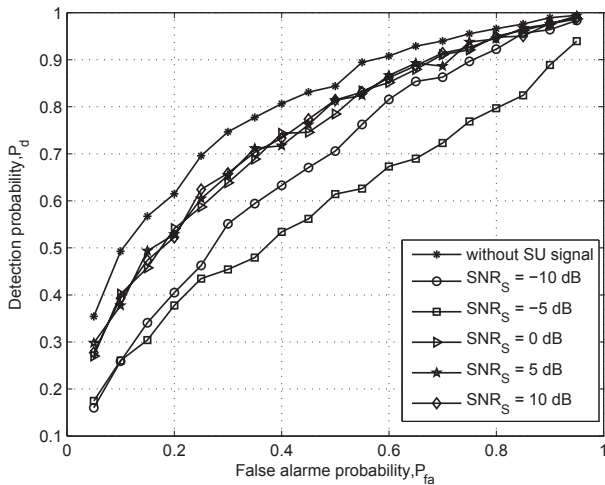


Fig. 5. ROC curves for the SAIC under variations of SU SNR.

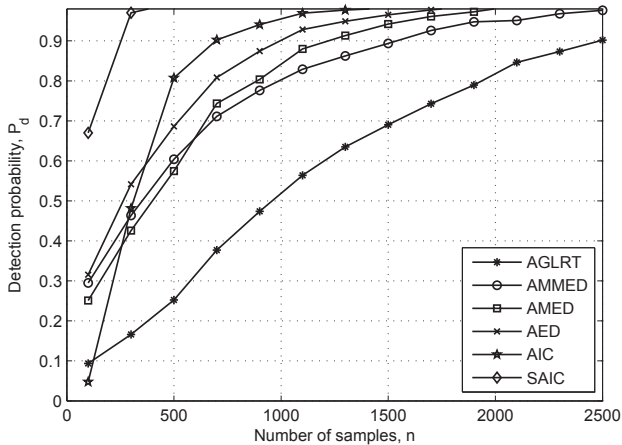


Fig. 6. P_d as a function of the number of samples for fixed $P_{fa} = 10\%$ and $SNR_S = 0$ dB.

the continuous sensing model, no matter the technique adopted.

Table II reports the required number of samples to reach $P_{fa} = 10\%$ e $P_d = 90\%$ for each technique and sensing model. For the AIC in the classical model, $n = 360$, which extrapolates the corresponding curve in Fig. 7.

TABLE II. NUMBER OF SAMPLES TO REACH A PROBABILITY OF FALSE ALARME OF 10% AND A PROBABILITY OF DETECTION OF 90%.

Technique	$SNR_S = 0$ dB	No SU signal
AGLRT	$n = 2480$	$n = 141$
AMMED	$n = 1550$	$n = 161$
AMED	$n = 1230$	$n = 84$
AED	$n = 1000$	$n = 125$
AIC	$n = 690$	$n = 360$
SAIC	$n = 260$	$n = 123$

The best performance of the AMED in terms of the number of samples in the classical model is consistent with the results

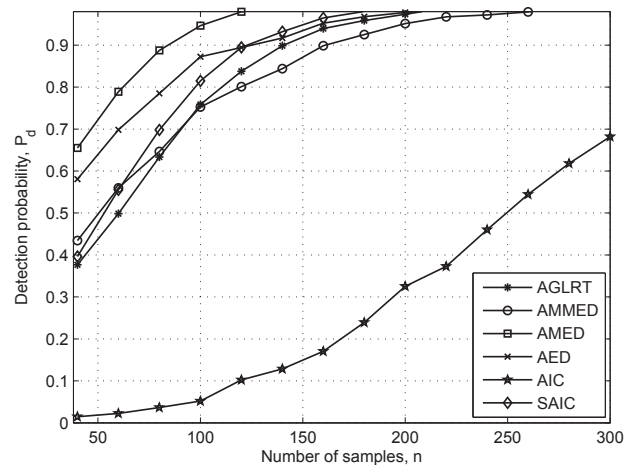


Fig. 7. P_d as a function of the number of samples for fixed $P_{fa} = 10\%$ and considering no transmission of SU signal.

in Fig. 7 and the ROC curves in Figs. 1–5. Its advantage is even more pronounced in comparison with the AED when a higher performance standard is set, e.g. when $P_{fa} = 10\%$ and $P_d = 90\%$. We notice that both the AMED and the AED have better performance than the AGLRT and the AMMED in classical or continuous sensing model. On the other hand, the AMED and the AED need a priori information about the power of noise and SU signal. In some circumstances, this information may not be available or can be unreliable. Unlike what is shown in Figs. 1–5, the AGLRT surpasses the AMMED in the classical model when $P_{fa} = 10\%$ and $P_d = 90\%$ is set. This is due to the fact that the AGLRT has higher statistical power [18]. However, the AGLRT is very inefficient for the continuous sensing model.

As observed from the ROC curves and Table II, SAIC has better performance than the four first techniques when a strong SU signal is present. This is because the stronger the SU signal, the shorter is the decision distance between the \mathcal{H}_0 and \mathcal{H}_1 states in the histogram of the decision variable. The AIC and SAIC try to estimate the number of sources directly and the bigger the SNR of all signals, the fewer is the incidence of error. However, the discrete nature of T_{AIC} limits its use only in friendly scenarios. We also notice that SAIC performs better than the AED under the classical model as well, unlike what is observed in the ROC curves. This proves that SAIC not only performs well in high interference condition, but also when there is no interference and high performance standards is required.

VI. CONCLUSION AND SUGGESTIONS FOR NEW RESEARCH

In this paper we compare the performances of eigenvalue spectrum sensing techniques in a multiple sensor cognitive radio network that uses the concept of continuous sensing and transmission. Using Monte Carlo simulations it was shown that the soft Akaike information criterion (SAIC) is the best option for detecting the PU signal when the SU signal is transmitting at the same time, and has good performance for the classical

model as well when $P_{fa} = 10\%$ and $P_d = 90\%$ is set. For the classical model, i.e. when there is no parallel transmission from secondary users, the AMED and the AED achieved the best results and can be used as the first choices if the noise power information is available. In spite of the moderate performance for the AMMED, its ROC curves showed that it is less sensitive to SU SNR variations. We confirmed what is stated in [14], that a longer sensing time for the continuous sensing model is needed to reach the same statistical performance as in the classical model, for a fixed bandwidth. This excess time may be prohibitive considering the channel coherence time and the bandwidth used to transmit all samples if a centralized cooperative multi-node system is employed. However, by choosing an appropriate technique, the effort may be less costly.

The scenarios with eigenvalue combining [21] and hard decision combining should be considered as candidates for applying the continuous sensing as well in future deployments of our proposal. Finally, the continuity of the work suggests a deeper analysis of the impact of other SU interference on the eigenvalue distribution of the sample covariance matrix and in turn the development of more suitable eigenvalue sensing strategy

REFERENCES

- [1] Shared Spectrum Company, *General Survey of Radio Frequency Bands - 30 MHz to 3 GHz*, 2010.
- [2] K. Harrison, S.M. Mishra, and A. Sahai, "How much white-space capacity is there?," in *2010 IEEE Symposium on New Frontiers in Dynamic Spectrum*, Singapore, pp. 1–10, Apr. 2010.
- [3] M. H. Islam, C. L. Koh, S. W. Oh, X. Qing, Y. Y. Lai, C. Wang, Y. C. Liang, B. E. Toh, F. Chin, G. L. Tan, and W. Toh, "Spectrum survey in Singapore: occupancy measurements and analysis," in *Proc. of CROWNCOM*, Singapore, May 2008.
- [4] Federal Communication Commission, *Report of spectrum efficiency working group*, Nov. 2002.
- [5] S. Haykin, Cognitive radio: brain-empowered wireless communications, *IEEE J. Sel. Areas Commun.*, vol. 23, no. 2, pp. 201–220, 2005.
- [6] Yücek, T., H. Arslan, "A survey of spectrum sensing algorithms for cognitive radio applications," *IEEE Commun. Surveys & Tutorials*, vol. 11, no. 1, pp. 116–129, 2009.
- [7] C. Cordeiro, K. Challapali, and D. Birru, "IEEE 802.22: An introduction to the first wireless standard based on cognitive radios," *Journal of Communications*, vol. 1, no. 1, 2006.
- [8] Y.-C. Liang, Y. Zeng, E. C. Y. Peh, and A. T. Hoang, "Sensing-throughput tradeoff for cognitive radio networks," *IEEE Trans. Wireless Commun.*, vol. 7, no. 4, pp. 1326–1337, 2008.
- [9] W. Y. Lee, I. F. Akyildiz, "Optimal spectrum sensing framework for cognitive radio networks," *IEEE Trans. Wireless Commun.*, vol. 7, no. 10, pp. 845–857, 2008.
- [10] E. Peh, Y.-C. Liang, Y. L. Guan, and Y. H. Zeng, "Optimization of cooperative sensing in cognitive radio networks: a sensing-throughput trade off view," *IEEE Trans. Veh. Technol.*, vol. 58, pp. 5294–5299, 2009.
- [11] A. Ghasemi and E. S. Sousa, "Optimization of spectrum sensing for opportunistic spectrum access in cognitive radio networks," in *Proc. 4th IEEE Consumer Commun. Networking Conf. (CCNC)*, pp. 1022–1026, 2007.
- [12] W. Hu, D. Willkomm, M. Abusubaih, J. Gross, G. Vlantis, M. Gerla, and A. Wolisz, "Dynamic frequency hopping communities for efficient IEEE 802.22 operation," *IEEE Commun. Mag.*, vol. 45, no. 5, pp. 80–87, 2007.
- [13] S. Boyd, M. Frye, M. Pursley, and T. Royster, "Spectrum monitoring during reception in dynamic spectrum access cognitive radio networks," *IEEE Trans. Commun.*, vol. 60, n. 2, pp. 547–558, 2012.
- [14] R. Bizerra, A. J. Braga, and G. Carvalho, "A spectrum sensing model for continuous transmission in cognitive radio network," in *Proc. Wireless Telecommunications Symposium (WTS)*, pp. 1–7, London, Apr. 2012.
- [15] H. Urkowitz, "Energy detection of unknown deterministic signals," in *Proc. IEEE*, vol. 55, pp. 523–531, 1967.
- [16] B. Nadler, F. Penna, and R. Garello, "Performance of eigenvalue-based signal detectors with known and unknown noise level," in *Proc. IEEE International Conference on Communications, ICC*, Kyoto, Japan, 5–9 June 2011; pp. 1–5.
- [17] M. Wax, and T. Kailath, "Detection of signals by information theoretic criteria," *IEEE Trans. Acoust., Speech, Signal Process.*, vol. 33, pp. 387–392, 1985.
- [18] D. A. Guimaraes, R. A. A. de Souza, and A. N. Barreto, "Performance of cooperative eigenvalue spectrum sensing with a realistic receiver under impulsive noise," *Journal of Sensor and Actuator Networks (JSAN)*, vol. 2, issue 1, pp. 46–69, 2013. Available: <http://www.mdpi.com/2224-2708/2/1/46>.
- [19] M. A. Hossain, R. Passerone, *Power Adaptive Cognitive Pilot Channel for Spectrum Co-existence in Wireless Networks*, in *Proc. IEEE International Conference on Advanced Information Networking and Applications (AINA)*, Singapore, Mar. 2011.
- [20] IEEE Standard for Information Technology–Telecommunications and information exchange between systems Wireless Regional Area Networks (WRAN)–Specific requirements Part 22: Cognitive Wireless RAN Medium Access Control (MAC) and Physical Layer (PHY) Specifications: Policies and Procedures for Operation in the TV Bands. *IEEE Std 802.22-2011*, 2011, pp. 1–680.
- [21] D. A. Guimaraes, C. R. N. da Silva and R. A. A. de Souza, "Cooperative spectrum sensing using eigenvalue fusion for OFDMA and other wideband signals," *Journal of Sensor and Actuator Networks (JSAN)*, vol. 2, issue 1, pp. 1–24, 2013. Available: <http://www.mdpi.com/2224-2708/2/1/1>.